

1 **Slow-down of Circumpolar Deepwater flow during the Late Neogene: Evidence from a**
2 **mudwave field at the Argentine continental slope**

3

4

5 Gruetzner, J.¹, Uenzelmann-Neben, G.¹, Franke, D.², Arndt, J.E.¹

6

7

8

9

10

11

12 ¹ Alfred-Wegener-Institut, Helmholtz-Zentrum für Polar- und Meeresforschung, Am Alten
13 Hafen 26, D-27568 Bremerhaven, Germany. (Jens.Gruetzner@awi.de, Gabriele.Uenzelmann-
14 Neben@awi.de, Jan.Erik.Arndt@awi.de)

15

16

17 ² Bundesanstalt für Geowissenschaften und Rohstoffe, Stilleweg 2, D-30655 Hannover,
18 Germany. (Dieter.Franke@bgr.de)

19

20 **Abstract**

21 Geochemical evidence from boreholes suggests enhanced transport of Northern Component
22 Water (NCW) to southern latitudes from about 6 Ma onwards. However, information on how
23 this change in transport influenced the intensity and position of current systems is sparse.
24 Here we use seismic reflection profiles interpreted together with bathymetric data to
25 investigate current derived deposits at the central Argentine Margin. Upslope migrating
26 mudwaves overlying a late Miocene erosional unconformity provide evidence that
27 Circumpolar Deepwater (CDW) flow slowed down with the onset of NCW inflow. During
28 the last ~3 Ma changes in dimensions and migration rates of the waves are small indicating
29 continuous bottom current flow conditions similar to today with only minor variations in flow
30 speed, suggesting that the Deep Western Boundary Current (DWBC) in the western south
31 Atlantic as observed today, has been a pervasive feature of the global thermohaline
32 circulation system during the Plio-/Pleistocene.

33

34

35 **Introduction**

36 During the late Neogene the Earth underwent a cooling trend interrupted only by a
37 subtle warming in the early Pliocene [*Zachos et al.*, 2001]. Changes in deep hydrography
38 associated with these transitions have been reconstructed from interbasinal carbon isotope
39 ($\delta^{13}\text{C}$) gradients [*Billups*, 2002; *Hodell and Venz-Curtis*, 2006; *Poore et al.*, 2006] and
40 Neodymium isotopes [*Klevenz et al.*, 2008] measured on sediments. A robust result of these
41 reconstructions is a major change at $\sim 7\text{-}6$ Ma indicating that nutrient-depleted Northern
42 Component Water (NCW) reached the southern hemisphere possibly due to the subsidence of
43 the Greenland Scotland Ridge (GSR) [*Poore et al.*, 2006; *Wright and Miller*, 1996] and/or the
44 closure of the Panamanian Gateway [*Billups*, 2002; *Haug and Tiedemann*, 1998]. Following
45 this event the relative proportion of NCW (%NCW) in the Southern Ocean was always
46 similar to or even exceeded the present day value. Further steps in $\delta^{13}\text{C}$ accompanied by
47 variations in %NCW occur at 2.8 and 1.6 Ma and were associated with the intensification of
48 Northern Hemisphere glaciations and a strong reduction in CDW ventilation during glacial
49 intervals [*Hodell and Venz-Curtis*, 2006].

50 The sensitivity in the deep ocean chemistry South Atlantic to fluctuations in %NCW
51 is high. Unfortunately drill cores providing continuous sediment records are sparse in this
52 area: Such records are particularly missing for the Argentine basin, a key area in global ocean
53 circulation where surface, intermediate and deep waters of southern origin are introduced into
54 the thermohaline cycle via a contour-following DWBC [*Smythe-Wright and Boswell*, 1998]

55 We here examine current derived deposits at the Argentine Margin, where a variety of
56 morphological features are diagnostic for along-slope sediment redistribution by the DWBC
57 [*Gruetzner et al.*, 2011; *Gruetzner et al.*, 2012; *Hernández-Molina et al.*, 2009; *Hernández-*
58 *Molina et al.*, 2010; *Krastel et al.*, 2011; *Preu et al.*, 2012]. In particular the location,
59 orientation and internal structure of a newly detected field of sediment waves (here called

60 mudwaves) at the middle slope allows insights into past variations in long-term bottom flow
61 activity from late Miocene to recent times.

62

63 **Oceanographic setting**

64 Surface and intermediate circulation encompasses the Brazil-Malvinas Confluence
65 (BMC), where the Falkland/Malvinas Current and the Brazil Current collide and mix (Fig. 1).
66 The confluence axis where both currents are deflected southward is located at 38-39°S on
67 average but seasonal variability of the BMC influences an area between 25°S and 45°S [*Piola*
68 *and Matano, 2001*].

69 In water depths of 1000-3500 m the DWBC consists of two CDW fractions: Upper
70 Circumpolar Deep Water (UCDW) and Lower Circumpolar Deep Water (LCDW; Fig.
71 1)[*Arhan et al., 2002*]. North of the BMC these two CDW fractions flow above (UCDW) and
72 below (LCDW) poleward directed NCW, which is formed in the high latitudes of the
73 Northern Hemisphere [*Piola and Matano, 2001*]. The interfaces between these water masses
74 as determined by density changes are at ~2000 m (UCDW/NCW) and at ~3500 m
75 (NCW/LCDW) but slightly deepen northward and are vertically displaced by eddies. South
76 of the BMC, today the NCW flows southward somewhat detached from the slope [*Memery et*
77 *al., 2000*]. At abyssal depths below 4000 m Antarctic Bottom Water (AABW) flows
78 northward in the DWBC and enters the Brazil Basin through the Vema and Hunter channels
79 [*Hogg et al., 1999*].

80

81 **Methods**

82 We interpreted 29 (7150 km) multi-channel seismic lines gathered by the Federal
83 Institute for Geosciences and Natural Resources (BGR) during two surveys (BGR87 and
84 BGR98) using the seismic vessels S.V. Explora and Akademik Lazarev, respectively. The

85 source volume ranged from 4258 in³ (69.8 l, BGR98) to 4906 in³ (80.4 l, BGR87), with
86 towed airgun arrays operating at a pressure of 2000 psi. All the seismic data were acquired
87 with a shot point interval of 50 m and a sampling rate of 4 ms. The streamer length during the
88 BGR87 and BGR98 cruises varied from 3000 to 4500 m, with 60 and 240 channels,
89 respectively. Details about the seismic processing can be found in *Franke et al.* [2010] and;
90 *Hinz et al.*, [1999]. We here use the seismostratigraphic model of [*Gruetzner et al.*, 2012].
91 Swath bathymetry data (HYDROSWEEP DS) from three cruises with R/V Meteor (M29/1,
92 M46/3, M49/2 [*Bleil et al.*, 2001; *Segl et al.*, 1994; *Spieß et al.*, 2002]) were jointly edited
93 with the software package QPS Fledermaus.

94

95 **Observations**

96 All investigated seismic profiles show the presence of sediment waves in the youngest
97 unit at the continental slope (Fig. 2, Fig. S1). Waveshapes are well developed and regular
98 between 42 and 43.5°S (Fig. 2b), while south of 43.5°S more irregular forms with variable
99 heights occur (Fig. 2d). The waves have spacings of 1.5 to 4 km and are 30 to 100 m high.
100 Regular waves show continuous curved internal reflectors converging smoothly towards the
101 seaward wave flanks (Fig. 2b). In contrast irregular waves often show abrupt termination of
102 the reflectors at both wave flanks (Fig. 2d). North of 43.5°S wave crests strike SSW-NNE at
103 ~28° while south of 43.5°S strike angles of 32-38° are observed (Fig. 2a,c). In the majority of
104 cases the wave profiles reveal an asymmetric morphology with a steeper western (upslope)
105 flank but shallower and smoother eastern (downslope) flank. Slight thickening of the upslope
106 flanks can be observed suggesting accretion on that side while at the downslope flanks less
107 deposition or erosion occurs (Fig. 2). As a result the sediment waves migrate upslope in a
108 WNW direction. The migrating sediment waves form an extensive field at a water depth of
109 2500 to 3500 m (Fig. 3) which is ~75 km wide and can be traced for 350 km within the

110 working area resulting in an area of $> 26000 \text{ km}^2$. The southward extension of the field is not
111 known since we do not have access to profiles to the south of the working area. However,
112 sediment waves can also be found within the same water depth range at 47.5°S to 48°S (Fig.
113 S1). A number of submarine canyons can be mapped that dissect the wave field in various
114 places (Fig. 3).

115 North of 43.5°S seismic section show buried waves directly overlying a strong
116 seismic reflector (Fig 2b). This late Miocene reflector (AR7 of [Gruetzner *et al.*, 2012]),
117 which can be traced throughout the working area, is discontinuous in some places on the
118 upper slope where canyons are intersecting but in the area of the wave field it is continuous.
119 The thickness of the wave field overlying AR7 is 550 – 1100 ms TWT (~ 600 to 900 m) with
120 decreasing values towards the North.

121 Another unconformity occurring at ~ 400 to 500 ms TWT below the sea floor (Fig. 2)
122 in most profiles subdivides the overlying unit and pinches out seaward at ~ 3.8 - 4.0 s TWT.
123 The local reflector, here called P, marks a change in depositional character with more regular
124 mudwaves developing above the unconformity.

125 Seaward of the wave field a plastered drift with a thickness of ~ 400 - 600 m and a
126 width of ~ 10 - 20 km can be traced for ~ 100 km within the working area [Gruetzner *et al.*,
127 2012]. The drift is also partly covered with sediment waves and terminates at about 43.5°S
128 where it is replaced northward by another wave field in a water depth range of 4000 to 5000
129 m (Figs. 3 and S1).

130

131 **Mudwave migration and bottom current flow**

132 Sedimentary waves are undulating depositional sedimentary structures that develop in
133 various environments where bottom flow patterns are stable over long periods of time [e.g.
134 Wynn *et al.*, 2000]. Wave dimensions and locations indicate that the wave field described

135 here could be either of bottom current origin (mudwaves) or developed under turbidity
136 currents [Wynn and Stow, 2002]. The shape of the field does not align with the downslope
137 pathways of major canyons (Fig. 3). Instead it is restricted to a margin parallel area in 2500 to
138 3500 m water depth. Waves occurring on landward levees of major canyons here migrate
139 away (upslope) from the canyon trough (Fig. S1), which is opposite to what is reported for
140 levees formed by turbidity current overflow [Carter *et al.*, 1990]. Also, a decrease in the rate
141 of wave growth over time is not observed. Such a decrease was found for sediment waves
142 bordering deepening channels with an increasing number of turbidites confined to the channel
143 [Carter *et al.*, 1990]. Furthermore, the sediment waves occur in the vicinity of a contourite
144 drift (Fig. 3) and are also observed in the same water depth range on bottom current shaped
145 slope terraces in the southern Argentine Basin (Fig. S1) [Gruetzner *et al.*, 2011; Hernández-
146 Molina *et al.*, 2009]. Sediment cores obtained within the mudwave area are mud/silt
147 dominated [Frenz *et al.*, 2004] with occasional sand layers. Physical property changes within
148 these sediments were attributed to climatic cycles and don't show comb type patterns with
149 many sharp spikes as typical for frequent distal turbiditic layers [Segl *et al.*, 1994]. Based on
150 these observations we conclude that the reported wave field was mainly shaped by bottom
151 currents and that turbidity current influence was only sporadic.

152 In the central Argentine basin mudwaves are widespread at the Zapiola Drift, and the
153 waves described here may be regarded as the mid-depth counterpart to large wave fields
154 generated by the AABW in depth > 4500 m [e.g. [Flood *et al.*, 1993; von Lom-Keil *et al.*,
155 2002]. But other than in the deep basin where mudwaves have been in existence since the
156 Late Oligocene [Manley and Flood, 1993], reflector AR7 gives good indication that wave
157 growth at the continental slope took place during Plio-Pleistocene.

158 Modeling studies [Blumsack and Weatherly, 1989] as well as empirical investigations
159 on mudwave fields [Flood *et al.*, 1993] suggest that, in the Southern Hemisphere, wave

160 migration should be commonly to the left of the flow direction. The observed upslope wave
161 migration in WNW direction at the Argentine slope is thus in agreement with a north setting
162 bottom current flow during the Plio-Pleistocene. Our results suggest a systematic change in
163 mudwave orientation at $\sim 43.5^{\circ}\text{S}$. Northward mudwaves align anti-clockwise ($\sim 6^{\circ}$) relative to
164 the regional contours (Fig. 2a) while further south wave crests strike up to $\sim 20^{\circ}$ clockwise
165 from the regional contours (Fig. 2c). It is difficult to infer current flow directions from the
166 strike of mud waves [Manley and Caress, 1994], especially when the waves are aligned
167 nearly parallel to the contours (a proxy for current direction) [Flood *et al.*, 1993]. However,
168 for the regular waves north of $\sim 43.5^{\circ}\text{S}$ theoretical models [Flood, 1988; Hopfauf *et al.*, 2001]
169 predict an upcurrent wave migration for a wide range (6 to 17 cm/s) of current velocities.

170

171 **Paleoceanographic implications**

172 The high amplitude seismic marker horizon AR7 was also identified in other studies
173 within the central Argentine margin and adjacent areas [Cavallotto *et al.*, 2011; Ewing and
174 Lonardi, 1971; Schümann, 2002; Violante *et al.*, 2010]. Based on a correlation with industry
175 well “Cruz del Sur” [Bushnell *et al.*, 2000] AR7 represents an unconformity close to the
176 Miocene/Pliocene boundary [Schümann, 2002]. Well “LAPA X-1” in the western Malvinas
177 basin [Galeazzi, 1998] and at DSDP Site 512 on the Maurice Ewing Bank [Ciesielski and
178 Weaver, 1983] show unconformities of approximately the same age. Furthermore, prominent
179 hiatuses are observed on the intermediate-depth Maurice Ewing Bank (MEB) located at the
180 eastern edge of the Falkland (Malvinas) Plateau with the major phase of erosion occurring
181 between 7.2 and 6.2 Ma (Fig. 4) [Ciesielski *et al.*, 1982], a time of widespread hiatuses in the
182 world oceans [Barron and Keller, 1982] affecting also the paleo-depth range between 2000
183 and 3500 m in the Atlantic [Keller and Barron, 1987]. At this time %NCW in the south
184 Atlantic was at a minimum [Billups, 2002; Poore *et al.*, 2006] possibly caused by a higher sill

185 depth of the GSR and a deep Panamanian gateway (Fig. 4). This implies that reflector AR7
186 represents the top of an erosional episode at the central Argentine margin which was caused
187 by vigorous bottom current circulation prior to the increase of NCW transport to the Southern
188 Ocean.

189 In the majority of the investigated reflection profiles north of 43.5°S buried sediment
190 waves of irregular shape directly overlie reflector AR7 which indicates that current velocities
191 shortly after ~ 6 Ma slowed down into a range where wave growth was possible at the slope.
192 This change correlates with a rapid increase in NCW production [Poore *et al.*, 2006] and a
193 sustained interval of high (three times the present day value) %NCW in the southern ocean
194 [Billups, 2002].

195 Unconformity P indicating a re-accelerated flow cannot be dated via direct borehole
196 correlation in the working area but may correlate to reflector “a”, a major regional
197 unconformity in the Weddell and Scotia Sea which was tentatively dated near the Early to
198 Late Pliocene boundary [Maldonado *et al.*, 2006]. Enhanced CDW flow at this time is also
199 indicated by limited deposition and widespread erosion and/or non-deposition over most of
200 the Maurice Ewing Bank from 4.0 to 3.2 Ma [Ciesielski *et al.*, 1982], a time, when %NCW at
201 ODP Site 1088 was at a local minimum [Billups, 2002] (Fig. 4).

202 North of 43.5°S regular waves indicate a stable CDW flow over the last ~3 Ma.
203 Utilizing a lee wave model [Flood, 1988] with the observed wave dimensions and the ratio of
204 downstream/upstream flank sedimentation rate (SRR) flow speeds estimated for 10 of these
205 regular waves yield current velocities of 7 to 17 cm/s which on average is slightly higher than
206 a current meter record from the slope (1970 m waterdepth) at ~38.5°S [Weatherly, 1993]. A
207 faster northward flow is indicated for the area south of 43.5°S by erosional features like
208 scours and moats. Thus the more regular waves occurring north of 43.5°S may point towards
209 a systematic northward decrease in speed of bottom water masses as noted on a larger scale

210 by [Hernández-Molina *et al.*, 2009] which may be due to the northward increasing interaction
211 of CDW with NCW.

212

213 **Conclusions**

214 A field of migrating mudwaves at 2500 – 3500 m water depth at the Argentine margin
215 that is described here for the first time and erosional unconformities allow inference of
216 changes in current intensity of CDW from the late Miocene (6 Ma) onward. Slow-downs of
217 the CDW towards moderate flow speeds as indicated by wave growth and migration are
218 found for time intervals with higher NCW inflow into the South Atlantic. In contrast, higher
219 current velocities causing hiatuses are associated with minima in %NCW. Differences in
220 wave shapes and orientations south and north of 43.5°S likely indicate stronger NCW
221 influence towards the North.

222

223

224 **Acknowledgement**

225 This research was funded by the Priority Program SAMPLE (South Atlantic Margin
226 Processes and Links with onshore Evolution) of the Deutsche Forschungsgemeinschaft
227 (DFG) under contract no. Ue 49/11 and Ue 49/15. We thank the anonymous reviewers and
228 editor MERIC SROKOSZ for their helpful comments.

229

230 **References**

- 231 Arhan, M., X. Carton, A. Piola, and W. Zenk (2002), Deep lenses of circumpolar water in the
232 Argentine Basin, *J. Geophys. Res.*, *107*(C1), 3007, doi: 10.1029/2001JC000963.
- 233 Barron, J. A., and G. Keller (1982), Widespread Miocene deep-sea hiatuses - coincidence
234 with periods of global cooling, *Geology*, *10*(11), 577-581, doi: 10.1130/0091-
235 7613(1982)10<577:WMDHCW>2.0.CO;2.
- 236 Billups, K. (2002), Late Miocene through early Pliocene deep water circulation and climate
237 change viewed from the sub-Antarctic South Atlantic, *Palaeogeogr. Palaeoclimatol.*
238 *Palaeoecol.*, *185*(3-4), 287-307, doi: 10.1016/S0031-0182(02)00340-1.
- 239 Bleil, U., and cruise participants (2001), Report and preliminary results of Meteor cruise M
240 46/3 Montevideo–Mar del Plata, 04.01.-07.02. 2000, *Ber. Fachb. Geowiss. Univ. Bremen*,
241 *172*.
- 242 Blumsack, S. L., and G. L. Weatherly (1989), Observations of the nearby flow and a model
243 for the growth of mudwaves, *Deep-Sea. Res.*, *36*(9), 1327-1339, doi: 10.1016/0198-
244 0149(89)90086-1.
- 245 Bushnell, D. C., J. E. Baldi, F. H. Bettini, H. Franzin, E. Kovaks, R. Marinelli, and G. J.
246 Wartenburg (2000), Petroleum system analysis of the Eastern Colorado Basin, offshore
247 Northern Argentina, in *Petroleum systems of South Atlantic margins*, edited by M. R.
248 Mello, pp. 403-415, AAPG Mem. 73.
- 249 Carter, L., R. M. Carter, C. S. Nelson, C. S. Fulthorpe, and H. L. Neil (1990), Evolution of
250 Pliocene to Recent abyssal sediment waves on Bounty Channel levees, New-Zealand, *Mar.*
251 *Geol.*, *95*(2), 97-109, doi: 10.1016/0025-3227(90)90043-J.
- 252 Cavallotto, J. L., R. A. Violante, and F. J. Hernández-Molina (2011), Geological aspects and
253 evolution of the Patagonian continental margin, *Biol. J. Linn. Soc.*, *103*(2), 346-362, doi:
254 10.1111/j.1095-8312.2011.01683.x.

255 Ciesielski, P. F., M. T. Ledbetter, and B. B. Ellwood (1982), The development of Antarctic
256 glaciation and the Neogene paleoenvironment of the Maurice Ewing Bank, *Mar. Geol.*,
257 46(1-2), 1-51, doi: 10.1016/0025-3227(82)90150-5.

258 Ciesielski, P. F., and F. M. Weaver (1983), Neogene and Quaternary paleoenvironmental
259 history of Deep Sea Drilling Project Leg 71 sediments, Southwest Atlantic Ocean, *Initial*
260 *Rep. Deep Sea Drill. Proj.*, 71, 461–477, doi:10.2973/dsdp.proc.71.120.1983.

261 Ewing, M., and A. G. Lonardi (1971), Sediment transport and distribution in the Argentine
262 Basin. 5. Sedimentary structure of the Argentine margin, basin, and related provinces, *Phys.*
263 *Chem. Earth.*, 8, 123-251, doi: 10.1016/0079-1946(71)90017-6.

264 Flood, R. D. (1988), A lee wave model for deep-sea mudwave activity, *Deep-Sea. Res.*,
265 35(6), 973-983, doi: 10.1016/0198-0149(88)90071-4.

266 Flood, R. D., A. N. Shor, and P. L. Manley (1993), Morphology of abyssal mudwaves at
267 Project MUDWAVES sites in the Argentine Basin, *Deep-Sea. Res. Pt. II*, 40(4-5), 859-888,
268 doi: 10.1016/0967-0645(93)90038-O.

269 Franke, D., S. Ladage, M. Schnabel, B. Schreckenberger, C. Reichert, K. Hinz, M. Paterlini,
270 J. de Aballeyra, and M. Siciliano (2010), Birth of a volcanic margin off Argentina, South
271 Atlantic, *Geochem. Geophys. Geosyst.*, 11(2), Q0AB04, doi: 10.1029/2009GC002715.

272 Frenz, M., R. Höppner, J. B. Stuu, T. Wagner, and R. Henrich (2004), Surface sediment bulk
273 geochemistry and grain-size composition related to the oceanic circulation along the South
274 American continental margin in the Southwest Atlantic, in *The South Atlantic in the Late*
275 *Quaternary*, edited by G. Wefer, et al., pp. 347-373, Springer.

276 Galeazzi, J. S. (1998), Structural and stratigraphic evolution of the western Malvinas Basin,
277 Argentina, *Am. Assoc. Pet. Geol. Bull.*, 82(4), 596–636.

278 Gruetzner, J., G. Uenzelmann-Neben, and D. Franke (2011), Variations in bottom water
279 activity at the southern Argentine margin: indications from a seismic analysis of a
280 continental slope terrace, *Geo-Mar. Lett.*, 31(5), 405-417, doi: 10.1007/s00367-011-0252-0.

281 Gruetzner, J., G. Uenzelmann-Neben, and D. Franke (2012), Variations in sediment transport
282 at the central Argentine continental margin during the Cenozoic, *Geochem. Geophys.*
283 *Geosyst.*, 13, Q10003, doi: 10.1029/2012GC004266

284 Haug, G. H., and R. Tiedemann (1998), Effect of the formation of the Isthmus of Panama on
285 Atlantic Ocean thermohaline circulation, *Nature*, 393(6686), 673-676, doi: 10.1038/31447.

286 Hernández-Molina, F. J., M. Paterlini, R. Violante, P. Marshall, M. de Isasi, L. Somoza, and
287 M. Rebesco (2009), Contourite depositional system on the Argentine Slope: An exceptional
288 record of the influence of Antarctic water masses, *Geology*, 37(6), 507-510, doi:
289 10.1130/g25578a.1.

290 Hernández-Molina, F. J., M. Paterlini, L. Somoza, R. Violante, M. A. Arecco, M. de Isasi, M.
291 Rebesco, G. Uenzelmann-Neben, S. Neben, and P. Marshall (2010), Giant mounded drifts
292 in the Argentine Continental Margin: Origins, and global implications for the history of
293 thermohaline circulation, *Mar. Petrol. Geol.*, 27(7), 1508-1530, doi:
294 10.1016/j.marpetgeo.2010.04.003.

295 Hinz, K., S. Neben, B. Schreckenberger, H. A. Roeser, M. Block, K. G. d. Souza, and H.
296 Meyer (1999), The Argentine continental margin north of 48°S: sedimentary successions,
297 volcanic activity during breakup, *Mar. Petrol. Geol.*, 16(1), 1-25, doi: 10.1016/S0264-
298 8172(98)00060-9.

299 Hodell, D. A., and K. A. Venz-Curtis (2006), Late Neogene history of deepwater ventilation
300 in the Southern Ocean, *Geochem. Geophys. Geosyst.*, 7(9), Q09001, doi:
301 10.1029/2005GC001211.

302 Hogg, N. G., G. Siedler, and W. Zenk (1999), Circulation and variability at the southern
303 boundary of the Brazil Basin, *J. Phys. Oceanogr.*, 29(2), 145-157, doi: 10.1175/1520-
304 0485(1999)029<0145:CAVATS>2.0.CO;2.

305 Hopfauf, V., V. Spieß, and Fachbereich Geowissenschaften (2001), A three-dimensional
306 theory for the development and migration of deep sea sedimentary waves, *Deep-Sea. Res.*
307 *Pt. I*, 48(11), 2497-2519, doi: 10.1016/S0967-0637(01)00026-7.

308 Keller, G., and J. A. Barron (1987), Paleodepth distribution of Neogene deep-sea hiatuses,
309 *Paleoceanography*, 2(6), 697-713, doi: 10.1029/PA002i006p00697.

310 Klevenz, V., D. Vance, D. N. Schmidt, and K. Mezger (2008), Neodymium isotopes in
311 benthic foraminifera: Core-top systematics and a down-core record from the Neogene south
312 Atlantic, *Earth Planet. Sci. Lett.*, 265(3-4), 571-587, doi: 10.1016/j.epsl.2007.10.053.

313 Krastel, S., G. Wefer, T. Hanebuth, A. Antobreh, T. Freudenthal, B. Preu, T. Schwenk, M.
314 Strasser, R. Violante, and D. Winkelmann (2011), Sediment dynamics and geohazards off
315 Uruguay and the de la Plata River region (northern Argentina and Uruguay), *Geo-Mar.*
316 *Lett.*, 31(4), 271-283, doi: 10.1007/s00367-011-0232-4.

317 Maldonado, A., F. Bohoyo, J. Galindo-Zaldívar, J. Hernández-Molina, A. Jabaloy, F. Lobo, J.
318 Rodríguez-Fernández, E. Suriñach, and J. Vázquez (2006), Ocean basins near the Scotia-
319 Antarctic plate boundary: Influence of tectonics and paleoceanography on the Cenozoic
320 deposits, *Mar. Geophys. Res.*, 27(2), 83-107, doi: 10.1007/s11001-006-9003-4.

321 Manley, P. L., and D. W. Caress (1994), Mudwaves on the Gardar Sediment Drift, NE
322 Atlantic, *Paleoceanography*, 9(6), 973-988, doi: 10.1029/94PA01755.

323 Manley, P. L., and R. D. Flood (1993), Paleoflow history determined from mudwave
324 migration - Argentine Basin, *Deep-Sea. Res. Pt. II*, 40(4-5), 1033-1055, doi: 10.1016/0967-
325 0645(93)90047-Q.

326 Memery, L., M. Arhan, X. A. Alvarez-Salgado, M. J. Messias, H. Mercier, C. G. Castro, and
327 A. F. Rios (2000), The water masses along the western boundary of the south and
328 equatorial Atlantic, *Prog. Oceanogr.*, 47(1), 69-98, doi: 10.1016/S0079-6611(00)00032-X.

329 Piola, A. R., and R. P. Matano (2001), Brazil and Falklands (Malvinas) Currents, in
330 *Encyclopedia of Ocean Sciences*, edited by J. H. Steele, et al., pp. 340-349, Academic
331 Press, London.

332 Poore, H. R., R. Samworth, N. J. White, S. M. Jones, and I. N. McCave (2006), Neogene
333 overflow of Northern Component Water at the Greenland-Scotland Ridge, *Geochem.*
334 *Geophys. Geosyst.*, 7, doi: 10.1029/2005GC001085.

335 Preu, B., T. Schwenk, F. J. Hernandez-Molina, R. Violante, M. Paterlini, S. Krastel, J.
336 Tomasini, and V. Spieß (2012), Sedimentary growth pattern on the northern Argentine
337 slope: The impact of North Atlantic Deep Water on southern hemisphere slope architecture,
338 *Mar. Geol.*, 329-331(0), 113-125, doi: 10.1016/j.margeo.2012.09.009.

339 Schümann, T. K. (2002), The hydrocarbon potential of the deep offshore along the Argentine
340 volcanic rifted margin - a numerical simulation, PhD thesis, 194 pp., RWTH Aachen,
341 Aachen, Germany.

342 Smythe-Wright, D., and S. Boswell (1998), Abyssal circulation in the Argentine Basin, *J.*
343 *Geophys. Res.*, 103(C8), 15845-15851, doi: 10.1029/98JC00142

344 Segl, M., and cruise participants (1994), Report and preliminary results of Meteor-cruise M
345 29/1: Buenos-Aires- Montevideo, 17.6. - 13.7.94, *Ber. Fachb. Geowiss. Univ. Bremen*, 94.

346 Spieß, V., and cruise participants (2002), Report and preliminary results of Meteor Cruise M
347 49/2, Montevideo (Uruguay)-Montevideo, 13.02.-07.03. 2001, *Ber. Fachb. Geowiss. Univ.*
348 *Bremen*, 84.

349 Violante, R. A., C. M. Paterlini, I. P. Costa, F. J. Hernández-Molina, L. M. Segovia, J. L.
350 Cavallotto, S. Marcolini, G. Bozzano, C. Laprida, N. García Chapori, T. Bickert, and V.

351 Spieß (2010), Sismoestratigrafía y evolución geomorfológica del talud continental
352 adyacente al litoral del este bonaerense, Argentina, *Latin American journal of*
353 *sedimentology and basin analysis*, 17(1), 33-62.

354 von Lom-Keil, H., V. Spieß, and V. Hopfauf (2002), Fine-grained sediment waves on the
355 western flank of the Zapiola Drift, Argentine Basin: evidence for variations in Late
356 Quaternary bottom flow activity, *Mar. Geol.*, 192(1-3), 239-258, doi: 10.1016/S0025-
357 3227(02)00557-1.

358 Weatherly, G. L. (1993), On deep-current and hydrographic observations from a mudwave
359 region and elsewhere in the Argentine Basin, *Deep-Sea. Res. Pt. II*, 40(4-5), 939-961, doi:
360 10.1016/0967-0645(93)90042-L.

361 Wright, J. D., and K. G. Miller (1996), Control of North Atlantic Deep Water circulation by
362 the Greenland-Scotland Ridge, *Paleoceanography*, 11(2), 157-170, doi:
363 10.1029/95PA03696.

364 Wynn, R. B., P. P. E. Weaver, G. Ercilla, D. A. V. Stow, and D. G. Masson (2000),
365 Sedimentary processes in the Selvage sediment-wave field, NE Atlantic: new insights into
366 the formation of sediment waves by turbidity currents, *Sedimentology*, 47(6), 1181-1197,
367 doi: 10.1046/j.1365-3091.2000.00348.x.

368 Wynn, R. B., and D. A. V. Stow (2002), Classification and characterisation of deep-water
369 sediment waves, *Mar. Geol.*, 192(1-3), 7-22, doi: 10.1016/S0025-3227(02)00547-9.

370 Zachos, J., M. Pagani, L. Sloan, E. Thomas, and K. Billups (2001), Trends, rhythms, and
371 aberrations in global climate 65 Ma to present, *Science*, 292(5517), 686-693, doi:
372 10.1126/science.1059412.

373

374

375 **Figure captions**

376 Figure 1. Study area with locations of seismic profiles and swath bathymetry. Inset shows
377 generalized present day oceanographic situation: AAIW = Antarctic Intermediate Water,
378 AABW = Antarctic Bottom Water; CDW = Circumpolar Deep Water and NCW = Northern
379 Component Water, MC = Malvinas Current, BC = Brazil Current, BMC = Brazil-Malvinas
380 Confluence. Black dot marks position of well “Cruz del Sur”.

381

382 Figure 2. Bathymetric and seismic images of mudwaves north (a, b) and south (c, d) of
383 43.5°S. Arrows in a and c indicate directions of regional contours, mudwave alignment and
384 wave migration.

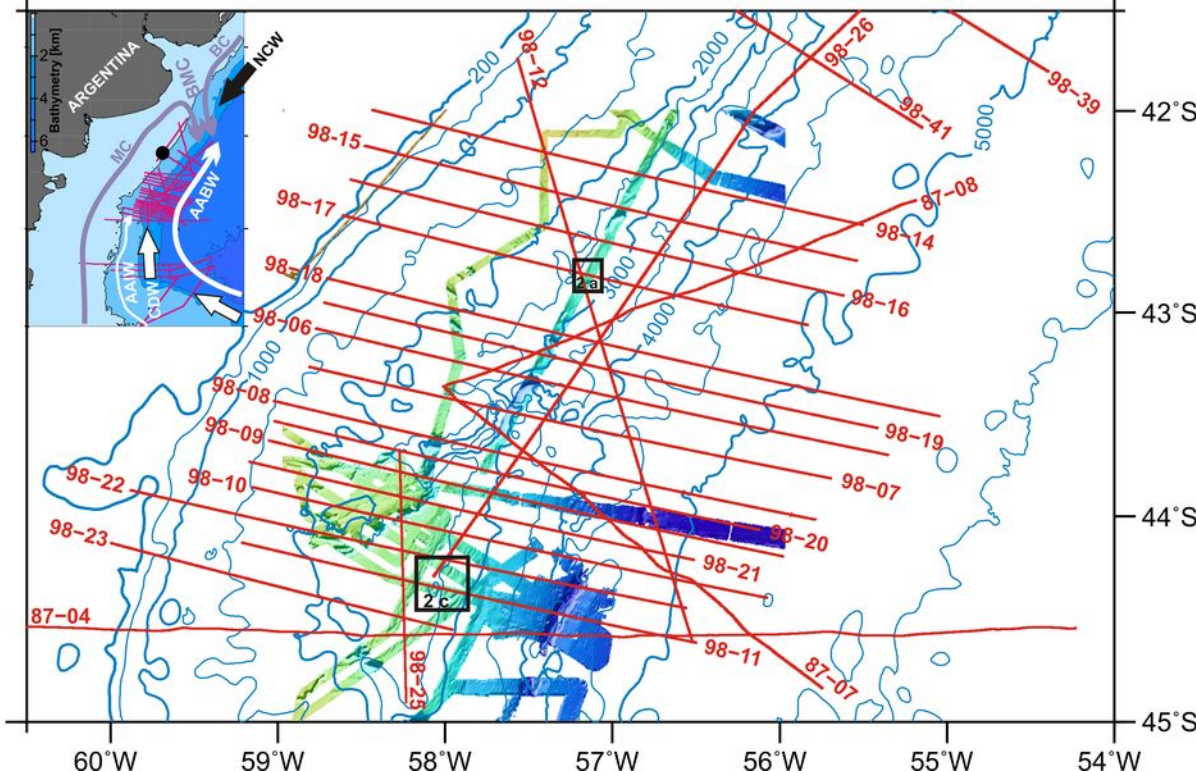
385

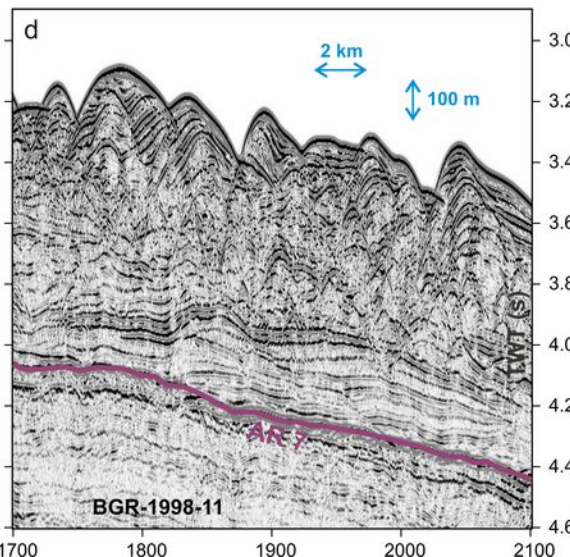
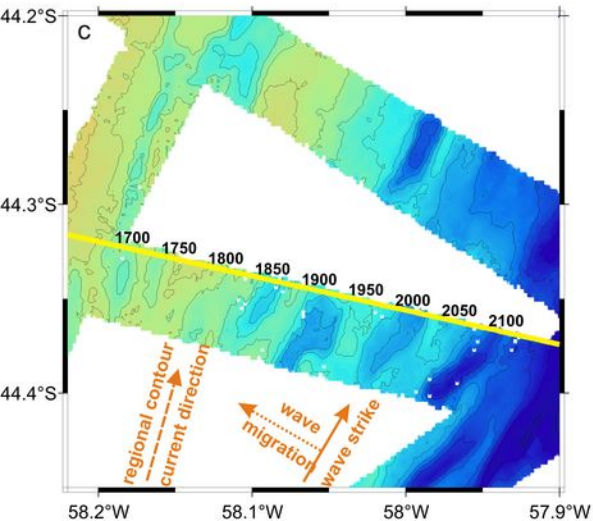
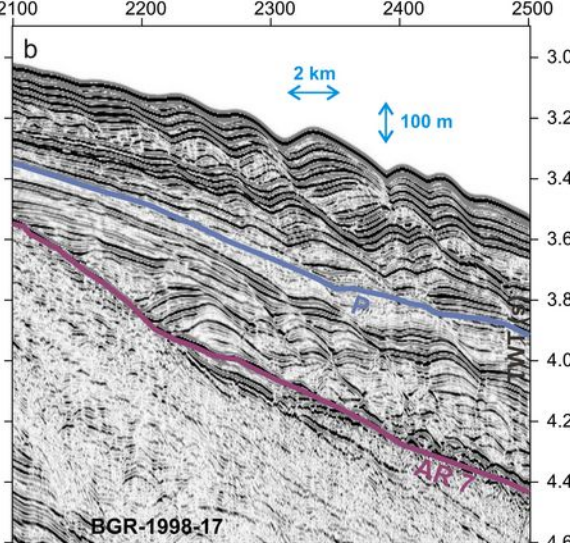
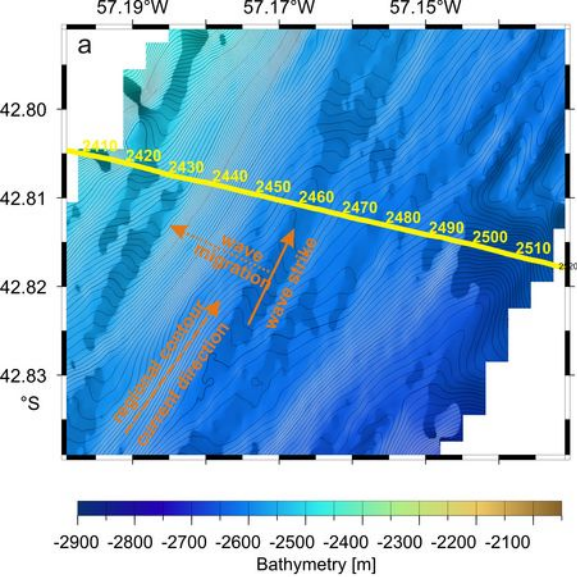
386 Figure 3. Bathymetric chart with location of mudwave fields and a contourite drift at the
387 Argentine margin. Arrows indicate bottom water flow: AABW = Antarctic Bottom Water;
388 CDW = Circumpolar Deep Water, NCW = Northern Component Water. Canyons are shown
389 in red. Contouritic channels are shown in orange.

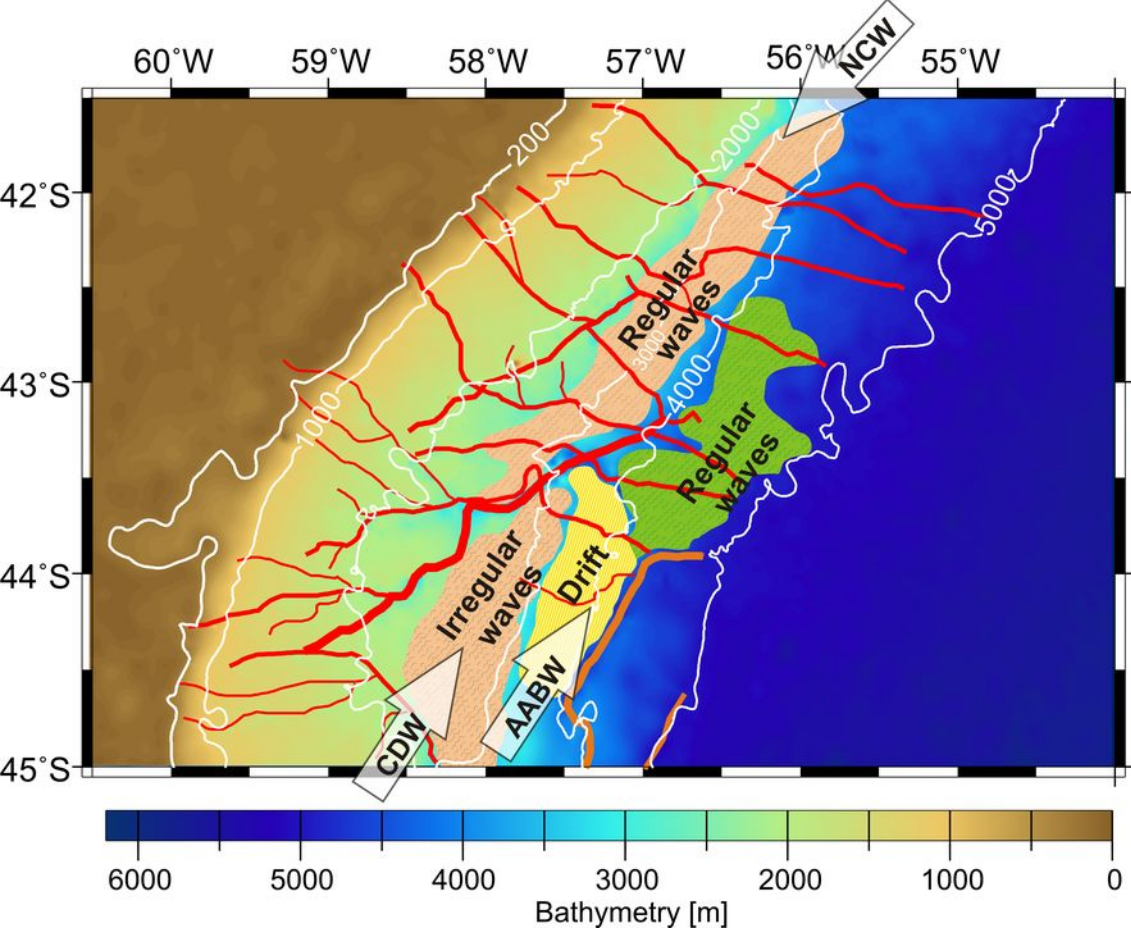
390

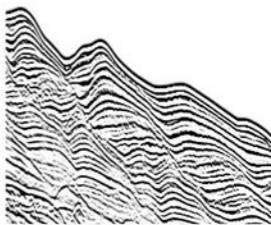
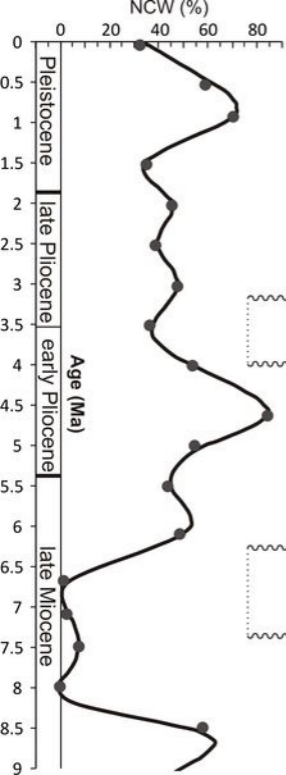
391 Figure 4. Evolution of erosional unconformities and mudwaves (right) in comparison to
392 occurrences of major hiatuses at the Maurice Ewing bank (center) [*Ciesielski et al.*, 1982] and
393 %NCW in the south Atlantic (left) [*Billups*, 2002].

394

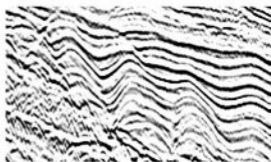








— P —



— AR 7 —